Available online at www.sciencedirect.com

SCIENCE DIRECT®

Biochimica et Biophysica Acta 1665 (2004) 29–39

BIOCHIMICA ET BIOPHYSICA ACTA
BBA

www.bba-direct.com

Influence of lipid chain unsaturation on membrane-bound melittin: a fluorescence approach

H. Raghuraman, Amitabha Chattopadhyay*

Centre for Cellular and Molecular Biology, Uppal Road, Hyderabad 500 007, India

Received 25 February 2004; received in revised form 8 June 2004; accepted 22 June 2004
Available online 23 July 2004

Abstract

Melittin, a cationic hemolytic peptide, is intrinsically fluorescent due to the presence of a single functionally important tryptophan residue. The organization of membrane-bound melittin is dependent on the physical state and composition of membranes. In particular, polyunsaturated lipids have been shown to modulate the membrane-disruptive action of melittin. Phospholipids with polyunsaturated acyl chains are known to modulate a number of physical properties of membranes and play an important role in regulating structure and function of membrane proteins. In this study, we have used melittin to address the influence of unsaturated lipids in modulating lipid–protein interactions. Our results show that fluorescence parameters such as intensity, emission maximum, polarization, lifetime and acrylamide quenching of melittin incorporated in membranes are dependent on the degree of unsaturation of lipids in membranes. Importantly, melittin in membranes composed of various unsaturated lipids shows red edge excitation shift (REES) implying that melittin is localized in a motionally restricted region in membranes. The extent of REES was found to increase drastically in membranes with increasing unsaturation, especially when the lipids contained more than two double bonds. In addition, increasing unsaturation in membranes causes a considerable change in the secondary structure of membrane-bound melittin. Taken together, our results assume significance in the overall context of the role of unsaturated lipids in membranes in the organization and function of membrane proteins and membrane-active peptides.

Keywords: Lipid–peptide interaction; Melittin; REES; Polyunsaturated lipid; Tryptophan fluorescence

1. Introduction

Melittin, the principal toxic component in the venom of the European honey bee, *Apis mellifera*, is a cationic hemolytic peptide [1]. It is a small linear peptide composed of 26 amino acids (NH_2-GIGAVLKVLTTGL-PALISWIKRKRQQ-$CONH_2$) in which the amino-terminal region (residues 1–20) is predominantly hydrophobic, whereas the carboxy terminal region (residues 21–26) is hydrophilic due to the presence of a stretch of positively charged amino acids. This amphiphilic property of melittin makes it water-soluble and yet it spontaneously associates with natural and artificial membranes. Such a sequence of amino acids, coupled with its amphiphilic nature, is characteristic of many membrane-bound peptides and putative transmembrane helices of membrane proteins [1]. This has resulted in melittin being used as a convenient model for monitoring lipid–protein interactions in membranes.

Despite the availability of a high resolution crystal structure of tetrameric melittin in aqueous solution [2],

Abbreviations: DMPC, 1,2-dimyristoyl-*sn*-glycero-3-phosphocholine; LUV, large unilamellar vesicle; MOPS, 3-(*N*-morpholino)propanesulfonic acid; PAPC, 1-palmitoyl-2-arachidonoyl-*sn*-glycero-3-phosphocholine; PDPC, 1-palmitoyl-2-docosahexaenoyl-*sn*-glycero-3-phosphocholine; PLPC, 1-palmitoyl-2-linoleoyl-*sn*-glycero-3-phosphocholine; POPC, 1-palmitoyl-2-oleoyl-*sn*-glycero-3-phosphocholine; REES, red edge excitation shift

* Corresponding author. Tel.: +91 40 2719 2578; fax: +91 40 2716 0311.
E-mail address: amit@ccmb.res.in (A. Chattopadhyay).

0005-2736/$ - see front matter © 2004 Elsevier B.V. All rights reserved.
doi:10.1016/j.bbamem.2004.06.008

the structure of the membrane-bound form is not yet resolved by X-ray crystallography. Yet, the importance of the membrane-bound form stems from the observation that the amphiphilic α-helical conformation of this hemolytic toxin in membranes resembles those of signal peptides [3], and the envelope glycoprotein gp41 from the human immunodeficiency virus (HIV) [4]. Furthermore, understanding melittin–membrane interaction assumes greater significance due to the recent finding that melittin mimics the N-terminal of HIV-1 virulence factor Nef1-25 [5].

Melittin is intrinsically fluorescent due to the presence of a single tryptophan residue, Trp-19, which makes it a sensitive probe to study the interaction of melittin with membranes and membrane-mimetic systems [6–9]. This is particularly advantageous since there are no other aromatic amino acids in melittin and this makes interpretation of fluorescence data less complicated due to lack of interference and heterogeneity. More importantly, it has been shown that the sole tryptophan residue of melittin is crucial for its powerful hemolytic activity [10]. The organization and dynamics of the tryptophan therefore become important for the function of the peptide. We have previously monitored the microenvironment experienced by the sole tryptophan in melittin when bound to membranes utilizing the wavelength-selective fluorescence approach. Our results show that the tryptophan residue is located in a motionally restricted region in the membrane [6,11] and the tryptophan environment is modulated by the surface charge of the membrane which could be related to the difference in the lytic activity of the peptide observed in membranes of varying charge [6].

Melittin has been widely used as a suitable model peptide for studying lipid–protein interactions due to its various modes of action with natural and model membranes [1]. It is well documented that the orientation (parallel or perpendicular to the plane of the membrane bilayer) and the lytic activity of melittin are dependent on the physical condition and the composition of the membrane to which it is bound [6,12–14]. In particular, it has been shown that lipid chain unsaturation modulates the lytic power [15] and bilayer micellization property [16] of melittin in membranes. These effects are dependent on the degree of unsaturation of the lipid acyl chains and the fraction of unsaturated lipids present in the membrane.

In this paper, we report the influence of lipid chain unsaturation on membrane-bound melittin utilizing fluorescence and circular dichroism (CD) spectroscopic approaches. We have previously shown that red edge excitation shift (REES) serves as a powerful tool to monitor the organization and dynamics of fluorescent probes and peptides/proteins bound to membranes and membrane mimetic media such as micelles and reverse micelles [6,8,9,11,17]. Our results assume significance in the overall context of the role of unsaturated lipids in membranes in the organization and function of membrane proteins and membrane-active peptides.

2. Materials and methods

2.1. Materials

Melittin of the highest available purity, and 3-(*N*-morpholino)propanesulfonic acid (MOPS) were obtained from Sigma Chemical Co. (St. Louis, MO, USA). 1-Palmitoyl-2-oleoyl-*sn*-glycero-3-phosphocholine (POPC), 1-palmitoyl-2-linoleoyl-*sn*-glycero-3-phosphocholine (PLPC), 1-palmitoyl-2-arachidonoyl-*sn*-glycero-3-phosphocholine (PAPC), 1-palmitoyl-2-docosahexaenoyl-*sn*-glycero-3-phosphocholine (PDPC) and 1,2-dimyristoyl-*sn*-glycero-3-phosphocholine (DMPC) were purchased from Avanti Polar Lipids (Alabaster, AL, USA). Lipids were checked for purity by thin layer chromatography on silica gel precoated plates (Sigma) in chloroform/methanol/water (65:35:5, v/v/v) and were found to give only one spot in all cases with a phosphate-sensitive spray and on subsequent charring [18]. The concentrations of phospholipids were determined by phosphate assay subsequent to total digestion by perchloric acid [19]. DMPC was used as an internal standard to assess lipid digestion. To avoid oxidation of polyunsaturated lipids, the stock solutions of these lipids were stored under argon at −20 °C. Any possible oxidation of polyunsaturated lipids was checked using a spectrophotometric assay [20] and no oxidative damage could be detected this way. The concentration of melittin in aqueous solution was calculated from its molar extinction coefficient (ε) of 5570 M^{-1} cm^{-1} at 280 nm [6]. Ultrapure grade acrylamide was from Gibco BRL (Rockville, MD, USA). The purity of acrylamide was checked from its absorbance using its molar extinction coefficient (ε) of 0.23 M^{-1} cm^{-1} at 295 nm and optical transparency beyond 310 nm [21]. All other chemicals used were of the highest purity available. Solvents used were of spectroscopic grade. Water was purified through a Millipore (Bedford, MA, USA) Milli-Q system and used throughout.

2.2. Sample preparation

All experiments were done using 100 nm diameter large unilamellar vesicles (LUVs) containing 2 mol% melittin. In general, 640 nmol (160 nmol for fluorescence quenching experiments) of lipid was dried under a stream of nitrogen while being warmed gently (~35 °C). After further drying under a high vacuum for not more than 3 h, 1.5 ml of 10 mM MOPS, 150 mM sodium chloride, 5 mM EDTA, pH 7.2 buffer was added, and the sample was vortexed under argon for 3 min to disperse the lipid and form homogeneous multilamellar vesicles. LUVs of 100 nm diameter were prepared by the extrusion technique using an Avestin Liposofast Extruder (Ottawa, Ontario, Canada) as previ-

ously described [22]. Briefly, the multilamellar vesicles were freeze–thawed five times using liquid nitrogen to ensure solute equilibration between trapped and bulk solutions, and then extruded through polycarbonate filters (pore diameter of 100 nm) mounted in the extruder fitted with Hamilton syringes (Hamilton Company, Reno, NV, USA). The samples were subjected to 11 passes through the polycarbonate filter to give the final LUV suspension. To incorporate melittin into membranes, a small aliquot containing 12.8 nmol (25.6 nmol for CD measurements) of melittin was added from a stock solution in water to the pre-formed vesicles and mixed well. For acrylamide quenching experiments, the total lipid used was less (4.8 nmol) to avoid scattering artifacts. Samples were incubated in the dark for 12 h under argon at room temperature (~23 °C) for equilibration before making measurements. Background samples were prepared the same way except that melittin was not added to them.

2.3. Steady state fluorescence measurements

Steady state fluorescence measurements were performed with a Hitachi F-4010 spectrofluorometer using 1 cm path length quartz cuvettes. Excitation and emission slits with a nominal bandpass of 5 nm were used for all measurements. All spectra were recorded using the correct spectrum mode. Background intensities of samples in which melittin was omitted were subtracted from each sample spectrum to cancel out any contribution due to the solvent Raman peak and other scattering artifacts. The spectral shifts obtained with different sets of samples were identical in most cases. In other cases, the values were within ±1 nm of the ones reported. Fluorescence polarization measurements were performed at room temperature (23 °C) using a Hitachi polarization accessory. Polarization values were calculated from the equation [23]:

$$P = \frac{I_{VV} - GI_{VH}}{I_{VV} + GI_{VH}} \quad (1)$$

where I_{VV} and I_{VH} are the measured fluorescence intensities (after appropriate background subtraction) with the excitation polarizer vertically oriented and emission polarizer vertically and horizontally oriented, respectively. G is the grating correction factor and is the ratio of the efficiencies of the detection system for vertically and horizontally polarized light, and is equal to I_{HV}/I_{HH}. All experiments were done with multiple sets of samples and average values of polarization are shown in Fig. 5.

2.4. Time-resolved fluorescence measurements

Fluorescence lifetimes were calculated from time-resolved fluorescence intensity decays using a Photon Technology International (London, Western Ontario, Canada) LS-100 luminescence spectrophotometer in the time-correlated single photon counting mode as described previously [8]. All experiments were performed using excitation and emission slits with a nominal bandpass of 4 nm or less. Fluorescence intensity decay curves so obtained were deconvoluted with the instrument response function and analyzed as a sum of exponential terms:

$$F(t) = \sum_i \alpha_i \exp(-t/\tau_i) \quad (2)$$

where $F(t)$ is the fluorescence intensity at time t and α_i is a pre-exponential factor representing the fractional contribution to the time-resolved decay of the component with a lifetime τ_i such that $\Sigma_i\ \alpha_i$=1. The decay parameters were recovered as described previously [8]. Mean (average) lifetimes $<\tau>$ for biexponential decays of fluorescence were calculated from the decay times and pre-exponential factors using the following equation [23]:

$$<\tau> = \frac{\alpha_1\tau_1^2 + \alpha_2\tau_2^2}{\alpha_1\tau_1 + \alpha_2\tau_2} \quad (3)$$

2.5. Fluorescence quenching measurements

Acrylamide quenching experiments of melittin tryptophan fluorescence in membranes of varying degrees of unsaturation were carried out by measurement of fluorescence intensity of melittin in separate samples containing increasing concentrations of acrylamide taken from a freshly prepared stock solution (8 M) in water. Samples were kept in the dark for 1 h before measuring fluorescence. The excitation wavelength used was 295 nm and emission was monitored at the fluorescence emission maximum of melittin in the given membrane system. Corrections for inner filter effect were made using the following equation [23]:

$$F = F_{obs}\text{antilog}[(A_{ex} + A_{em})/2] \quad (4)$$

where F is the corrected fluorescence intensity and F_{obs} is the background subtracted fluorescence intensity of the sample. A_{ex} and A_{em} are the measured absorbance at the excitation and emission wavelengths. The absorbance of the samples was measured using a Hitachi U-2000 UV–visible absorption spectrophotometer. Quenching data were analyzed by fitting to the Stern–Volmer equation [23]:

$$F_o/F = 1 + K_{SV}[Q] = 1 + k_q\tau_o[Q] \quad (5)$$

where F_o and F are the fluorescence intensities in the absence and presence of the quencher, respectively, $[Q]$ is the molar quencher concentration and K_{SV} is the Stern–Volmer quenching constant. The Stern–Volmer quenching constant K_{SV} is equal to $k_q\tau_o$ where k_q is the bimolecular quenching constant and τ_o is the lifetime of the fluorophore in the absence of quencher.

2.6. CD measurements

CD measurements were carried out at room temperature (23 °C) in a JASCO J-715 spectropolarimeter which was calibrated with (+)-10-camphorsulfonic acid. The spectra were scanned in a quartz optical cell with a path length of 0.1 cm. All spectra were recorded in 0.2 nm wavelength increments with a 4 s response and a band width of 1 nm. For monitoring changes in secondary structure, spectra were scanned in the far-UV range from 205 to 250 nm at a scan rate of 50 nm/min. Each spectrum is the average of 15 scans with a full-scale sensitivity of 50 mdeg. All spectra were corrected for background by subtraction of appropriate blanks and were smoothed making sure that the overall shape of the spectrum remains unaltered. Data are represented as molar ellipticities and were calculated using the equation:

$$[\theta] = \theta_{obs}/(10\ Cl) \quad (6)$$

where θ_{obs} is the observed ellipticity in mdeg, l is the path length in cm, and C is the melittin concentration in mol/l.

3. Results

Fig. 1 shows the chemical structures of the unsaturated phospholipids used in this study. We chose zwitterionic phosphatidylcholine as the phospholipid headgroup to ensure that there is minimal electrostatic interaction with the cationic peptide melittin. Further, we chose mixed acyl chain phospholipids since most biological membranes are composed of phospholipids which are predominantly saturated at the *sn*-1 position, and unsaturated at the *sn*-2 position [24]. These mixed acyl chain phospholipids remain in the biologically relevant fluid phase at physiological temperatures due to their low phase transition temperatures. The phospholipids used are chosen such that the *sn*-1 acyl chain is saturated (16:0), whereas the *sn*-2 acyl chain is unsaturated with the extent of unsaturation increasing in the order POPC (18:1), PLPC (18:2), PAPC (20:4), and PDPC (22:6). The gradual variation of the number of double bonds in the *sn*-2 position keeping the fatty acyl chain composition in the *sn*-1 position invariant, sets up an appropriate condition to monitor the effect of degree of unsaturation in membranes on the organization and dynamics of membrane-bound melittin.

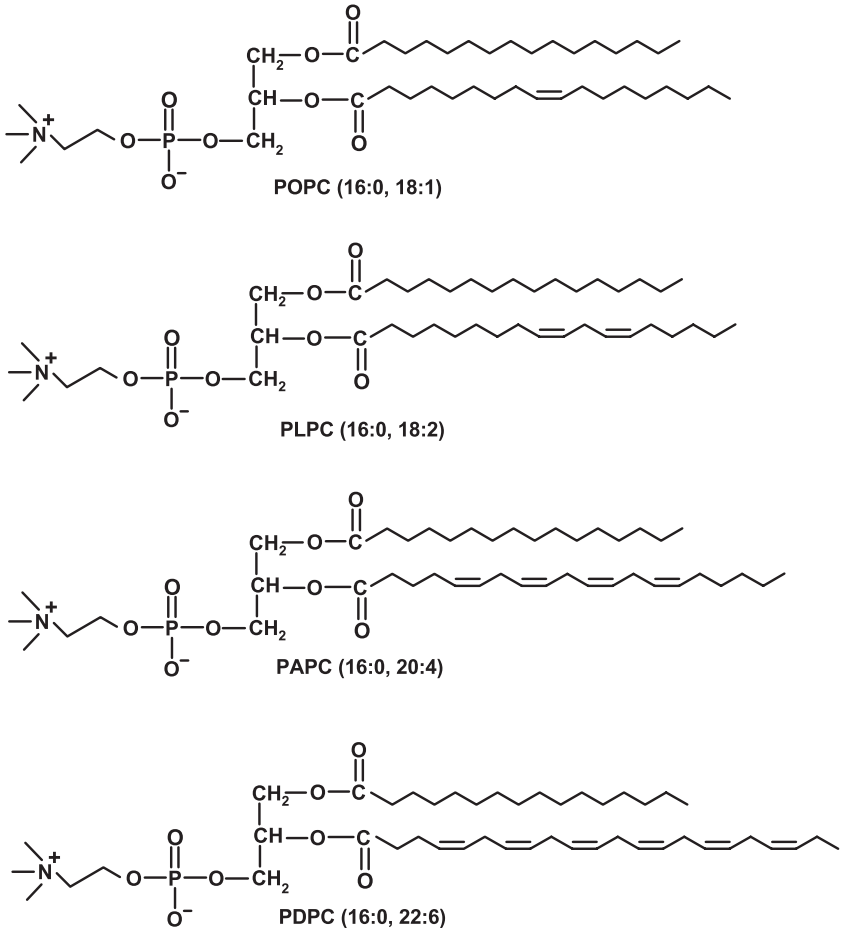

Fig. 1. Chemical structures of the unsaturated phospholipids used. The composition of the acyl chains is indicated in parentheses.

3.1. Fluorescence of membrane-bound melittin

The fluorescence emission maximum of melittin bound to monounsaturated POPC membranes is 337 nm when excited at 280 nm. The magnitude of the emission maximum is indicative of the membrane interfacial localization of the tryptophan residue in melittin [6,11]. The fluorescence emission maximum of membrane-bound melittin exhibits a small red shift in membranes composed of polyunsaturated phospholipids. Thus, the emission maximum of melittin bound to PLPC, PAPC and PDPC membranes is 337, 338 and 339 nm, respectively. The red shift of the emission maximum with increasing unsaturation could be due to an increased water content in these membranes [25,26].

As shown in Fig. 2, the fluorescence intensity of melittin shows reduction with increasing phospholipid unsaturation which is apparent only for PAPC (four double bonds) and PDPC (six double bonds) membranes. Tryptophan fluorescence intensity is sensitive to the presence of water in its immediate environment since water is known to quench tryptophan fluorescence [8]. The decrease (~20%) in the fluorescence intensity observed in PAPC and PDPC membranes could therefore be due to the increased water content of these membranes resulting in an increased polarity around the tryptophan residue. The decrease in fluorescence intensity of melittin is more pronounced when the number of double bonds is changed from two to four beyond which there is no significant change in the fluorescence intensity of membrane-bound melittin.

3.2. REES of melittin in membranes composed of varying degrees of unsaturation

REES represents a powerful approach which can be used to directly monitor the environment and dynamics around a fluorophore in a complex biological system [17]. A shift in the wavelength of maximum fluorescence emission toward higher wavelengths, caused by a shift in the excitation wavelength toward the red edge of the absorption band, is termed REES. This effect is mostly observed with polar fluorophores in motionally restricted media such as viscous solutions or condensed phases where the dipolar relaxation time for the solvent shell around a fluorophore is comparable to or longer than its fluorescence lifetime [17,27]. REES arises from slow rates of solvent relaxation (reorientation) around an excited state fluorophore which depends on the motional restriction imposed on the solvent molecules in the immediate vicinity of the fluorophore. Utilizing this approach, it becomes possible to probe the mobility parameters of the environment itself (which is represented by the relaxing solvent molecules) using the fluorophore merely as a reporter group. Further, since the ubiquitous solvent for biological systems is water, the information obtained in such cases will come from the otherwise 'optically silent' water molecules.

The unique feature about REES is that while all other fluorescence techniques (such as fluorescence quenching, energy transfer, and polarization measurements) yield information about the fluorophore (either intrinsic or extrinsic) itself, REES provides information about the relative rates of solvent (water in biological systems) relaxation dynamics which is not possible to obtain by other techniques. This makes REES extremely useful since hydration plays a crucial modulatory role in a large number of important cellular events including protein folding, lipid–protein interactions and ion transport [28].

The shifts in the maxima of fluorescence emission[1] of the tryptophan residue of melittin, bound to membranes of unsaturated phospholipids, as a function of excitation wavelength are shown in Fig. 3a. As the excitation wavelength is changed from 280 to 307 nm, the emission maxima of membrane-bound melittin are shifted from 337 to 344 nm (in POPC), 337 to 345 nm (PLPC), 339 to 356 nm (PAPC), and 339 to 358 nm (PDPC). This corresponds to REES of 7, 8, 17, and 19 nm for melittin bound to membranes of POPC, PLPC, PAPC, and PDPC, respectively. Such dependence of the emission maximum on excitation wavelength is characteristic of REES. This implies that the tryptophan residue in melittin is localized in a motionally restricted region of the membrane in these cases. This is consistent with the interfacial localization of the melittin tryptophan when bound to membranes [6,11]. The membrane interface is characterized by unique motional

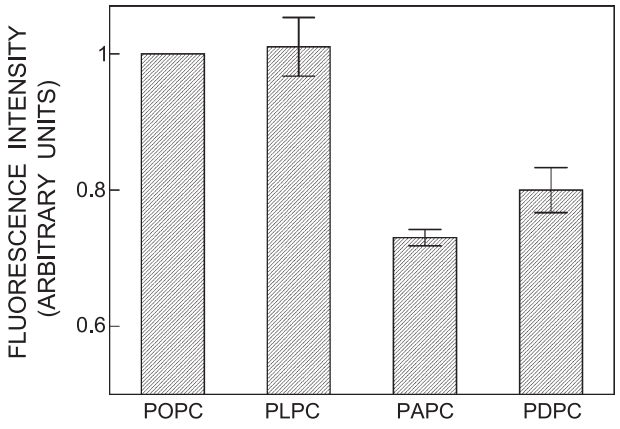

Fig. 2. Effect of increasing number of double bonds at the *sn*-2 fatty acyl chain on the fluorescence intensity of melittin bound to membranes of varying degrees of unsaturation. Excitation wavelength used was 280 nm and emission was collected at 337 nm. The data points shown are the means±S.E. of three independent measurements. The ratio of melittin to lipid was 1:50 (mol/mol) and the concentration of melittin was 8.53 μM in all cases. See Materials and methods for other details.

[1] We have used the term maximum of fluorescence emission in a somewhat wider sense here. In every case, we have monitored the wavelength corresponding to maximum fluorescence intensity, as well as the center of mass of the fluorescence emission. In most cases, both these methods yielded the same wavelength. In cases where minor discrepancies were found, the center of mass of emission has been reported as the fluorescence maximum.

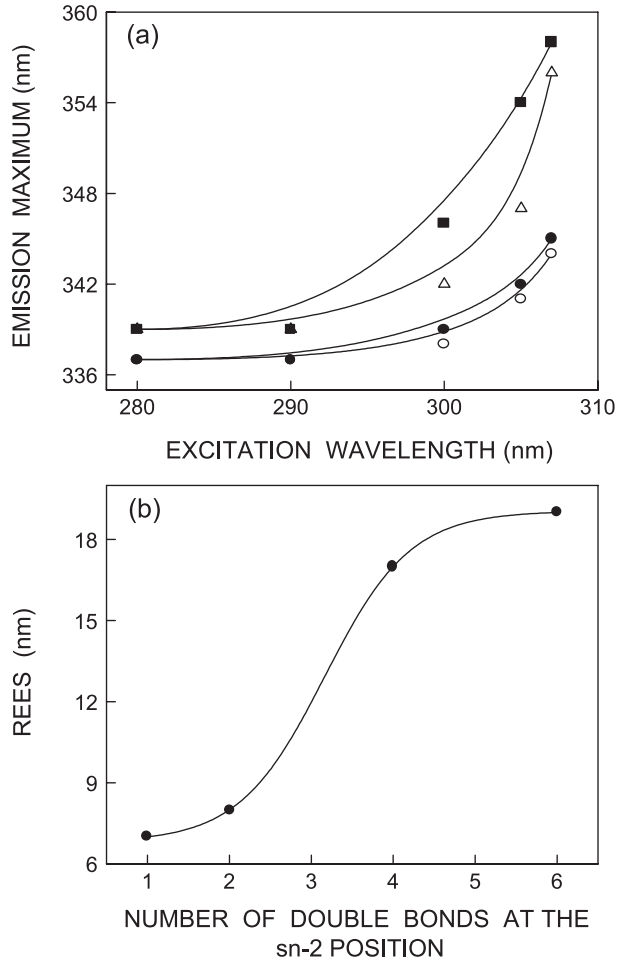

Fig. 3. (a) Effect of changing excitation wavelength on the wavelength of maximum emission of melittin bound to membranes of varying degrees of unsaturation corresponding to POPC (○), PLPC (●), PAPC (△), and PDPC (■). (b) Effect of increasing number of double bonds at the *sn*-2 fatty acyl chain of the unsaturated phospholipid on the magnitude of REES of melittin bound to membranes of varying degrees of unsaturation. REES data obtained from panel a is plotted as a function of increasing number of double bonds at the *sn*-2 fatty acyl chain of phospholipids. All other conditions are as in Fig. 2. See Materials and methods for other details.

and dielectric characteristics distinct from both the bulk aqueous phase and the more isotropic hydrocarbon-like deeper regions of the membrane [17,29]. This specific region of the membrane exhibits slow rates of solvent relaxation and is also known to participate in intermolecular charge interactions and hydrogen bonding through the polar headgroup. These structural features which slow down the rate of solvent reorientation have previously been recognized as typical features of microenvironments giving rise to significant REES effects. It is therefore the membrane interface which is most likely to display red edge effects [17].

Interestingly, the magnitude of REES appears to be dependent on the extent of unsaturation in the membrane as shown in Fig. 3b. Melittin exhibits REES of 7–8 nm in membranes of mono- and diunsaturated (POPC and PLPC) phospholipids. There is a drastic increase in the magnitude of REES when the number of double bonds is increased beyond two. Thus, melittin in PAPC and PDPC membranes displays REES of 17 and 19 nm, respectively. These results show that the immediate environment around the tryptophan, in terms of dynamics (rate of solvent reorientation) of hydration, changes with increasing unsaturation in the *sn*-2 fatty acyl chain. In particular, the change is more apparent from PLPC to PAPC which shows a large change in REES. This is consistent with the previous observation that in fatty acyl chains with more than two *cis* double bonds, there is a significant increase in water permeability [25,26], possibly due to the disordering of the membrane associated with it [30]. It is worth mentioning here that the magnitude of REES obtained with melittin in PAPC and PDPC membranes are considerably higher than what is usually reported for membrane-bound tryptophan residues [6,11,31] although higher REES have been reported in a few cases [32,33].

3.3. Fluorescence lifetime and polarization measurements of membrane-bound melittin

It is well known that fluorescence lifetime of tryptophan in particular is sensitive to solvent, temperature and excited state interactions [34]. A typical decay profile of tryptophan residue of membrane-bound melittin with its biexponential fitting and the statistical parameters used to check the goodness of the fit is shown in Fig. 4a.

The fluorescence lifetimes of melittin bound to membranes with varying degrees of unsaturation are shown in Table 1. As seen from the table, all fluorescence decays could be fitted well with a biexponential function. The mean fluorescence lifetimes were calculated using Eq. (3) and are shown in Fig. 4b. As shown in the figure, there is an overall decrease (~16%) in mean fluorescence lifetime of melittin with increasing acyl chain unsaturation. The shortening of lifetime could possibly be due to increased water penetration in the interfacial region of membranes due to increasing unsaturation and altered packing of the phospholipid fatty acyl chains. In general, an increase in polarity of the tryptophan environment is known to reduce the lifetime of tryptophans due to fast deactivating processes in polar environments [34]. With an increase in the number of double bonds in the *sn*-2 fatty acyl chain, the polarity of the tryptophan environment would increase due to increased water penetration induced by the presence of polyunsaturation [25,26] resulting in a reduction in lifetime. This is consistent with the observation of reduction in fluorescence intensity of membrane-bound melittin with increasing unsaturation (Fig. 2). Interestingly, the change in mean fluorescence lifetime is more prominent when the number of double bonds is increased from two to four, in agreement with the fluorescence intensity and REES results described above (Figs. 2 and 3b).

The fluorescence polarization of membrane-bound melittin is shown in Fig. 5. The polarization values show a steady decrease with increasing number of double bonds in the

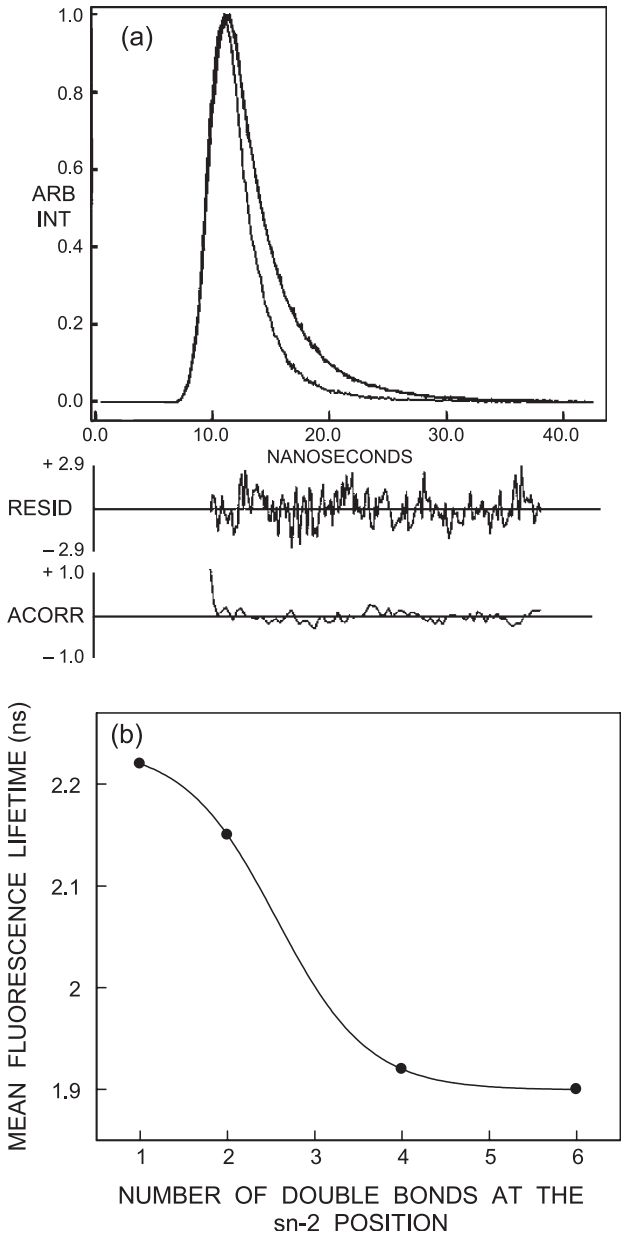

Fig. 4. (a) Time-resolved fluorescence intensity decay of melittin bound to POPC membranes. Excitation wavelength was at 297 nm which corresponds to a peak in the spectral output of the nitrogen lamp. Emission was monitored at 337 nm. The sharp peak on the left is the lamp profile. The relatively broad peak on the right is the decay profile, fitted to a biexponential function. The two lower plots show the weighted residuals and the autocorrelated function of the weighted residuals. (b) Effect of increasing number of double bonds at the *sn*-2 fatty acyl chain on mean fluorescence lifetime of melittin bound to membranes of varying degrees of unsaturation. Mean fluorescence lifetimes were calculated from Table 1 using Eq. (3). The excitation wavelength used was 297 nm, and emission was set at 337 nm. All other conditions are as in Fig. 2. See Materials and methods for other details.

fatty acyl chain. This indicates that the rotational mobility of melittin is considerably increased in polyunsaturated membranes and the increase is more pronounced when the degree of unsaturation in membranes is higher. It has been reported earlier that poly-*cis* unsaturated lipid bilayers are more

Table 1
Lifetimes of melittin bound to membranes composed of varying degrees of unsaturation[a]

Lipid	α_1	τ_1 (ns)	α_2	τ_2 (ns)
POPC	0.12	4.17	0.88	0.76
PLPC	0.11	4.27	0.89	0.90
PAPC	0.10	3.97	0.90	0.83
PDPC	0.12	3.63	0.88	0.73

[a] The excitation wavelength was 297 nm; emission was monitored at 337 nm. All other conditions are as in Fig. 2. See Materials and methods for other details.

flexible than membranes made of their saturated or monounsaturated counterparts [35]. Further, an increased 'free volume' at the membrane interfacial region (where the sole tryptophan of melittin is localized) has been suggested for membranes containing unsaturated phospholipids [36]. These factors could account for the reduction in fluorescence polarization observed with increasing unsaturation in the membrane.

In order to ensure that the polarization values measured for membrane-bound melittin are not influenced by lifetime-induced artifacts, the apparent (average) rotational correlation times were calculated using Perrin's equation [8]:

$$\tau_c = \frac{<\tau> r}{r_o - r} \quad (8)$$

where r_o is the limiting anisotropy of tryptophan, r is the steady state anisotropy (derived from the polarization values using $r=2P/(3-P)$), and $<\tau>$ is the mean fluorescence lifetime taken from Fig. 4b. The values of the apparent rotational correlation times, calculated this way using a value of r_o of 0.09 [8], are shown in Fig. 5. As is evident from the figure, the apparent rotational correlation times show progressive decrease with increase in mem-

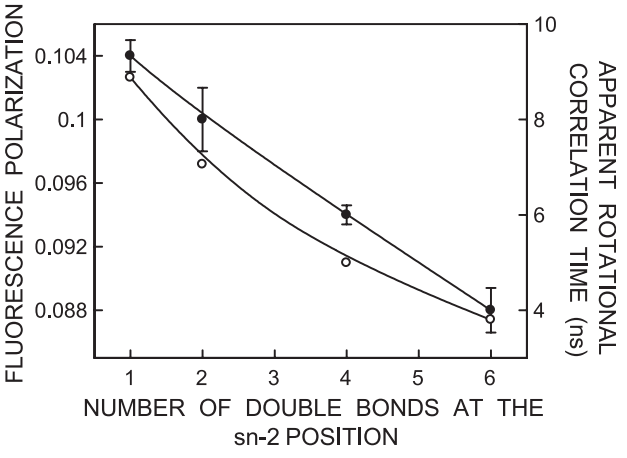

Fig. 5. Effect of increasing number of double bonds at the *sn*-2 fatty acyl chain on the fluorescence polarization (●) and apparent rotational correlation times (○) of melittin bound to membranes of varying degrees of unsaturation. The data points shown are the means±S.E. of three independent measurements. All other conditions are as in Fig. 2. See Materials and methods for other details.

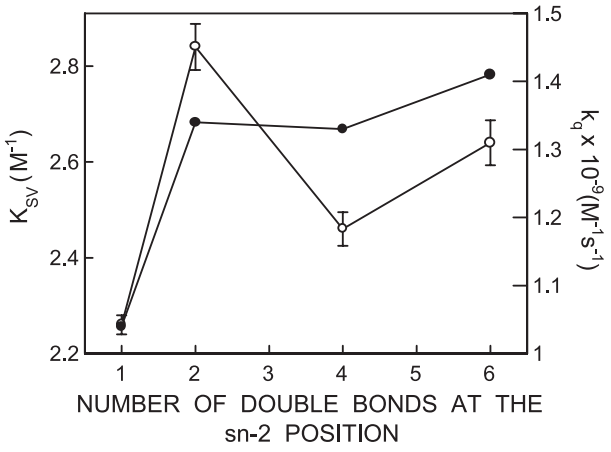

Fig. 6. Stern–Volmer quenching constants, K_{SV} (○) and bimolecular quenching constants, k_q (●) for acrylamide quenching of melittin bound to membranes of varying degrees of unsaturation. The bimolecular quenching constants were calculated using Eq. (5). The excitation wavelength was 295 nm and emission was monitored at 337 nm. The data points shown are the means±S.E. of three independent measurements. The ratio of melittin to lipid was 1:50 (mol/mol) and the concentration of melittin was 3.2 μM in all cases. See Materials and methods for other details.

brane unsaturation and therefore parallels the trend observed with fluorescence polarization of membrane-bound melittin. This clearly shows that the observed changes in polarization values are free from lifetime-induced artifacts.

3.4. Acrylamide quenching of melittin tryptophan fluorescence

The above results show that increasing acyl chain unsaturation in membranes enhances the polarity of the interfacial region of membranes due to increased water penetration. Previous literature reports have rationalized such observations by the fact that a membrane bilayer with increased free volume in the interfacial region would be more permeable to small molecules such as water [36]. We performed fluorescence quenching experiments using acrylamide to explore this issue further and to examine the accessibility and relative location of melittin in membranes of varying degrees of unsaturation. Acrylamide is a widely used neutral aqueous quencher of tryptophan fluorescence [21]. The slope of the Stern–Volmer plot, obtained from acrylamide quenching experiments, is the Stern–Volmer constant (K_{SV}). This parameter (K_{SV}) is related to the degree of exposure (accessibility) of the melittin tryptophan to the aqueous phase. In general, the higher the value of K_{SV}, the greater the degree of exposure, assuming that there is not a large difference in fluorescence lifetime. The quenching parameter (K_{SV}) obtained by analyzing the Stern–Volmer plots is shown in Fig. 6. Surprisingly, there is no apparent correlation between the accessibility of the melittin tryptophan to the aqueous phase to the increasing acyl chain unsaturation. However, the bimolecular quenching constant (k_q) is a more accurate measure of the degree of exposure since it takes into account the differences in fluorescence lifetime (see Eq. (5)). The k_q values, calculated using mean fluorescence lifetimes from Fig. 4b and Eq. (5), are shown in Fig. 6. It is somewhat reassuring to note that the overall accessibility of melittin tryptophan is higher in polyunsaturated membranes when compared to monounsaturated membranes, when judged by changes in k_q values. Nonetheless, this trend in accessibility did not compare well with changes in fluorescence parameters such as intensity (Fig. 2), REES (Fig. 3b), and lifetime (Fig. 4b) with increasing membrane unsaturation. The reason for this apparent discrepancy is not clear.

3.5. Effect of increasing acyl chain unsaturation on the secondary structure of membrane-bound melittin

To investigate the effect of increasing acyl chain unsaturation on the secondary structure of melittin, we carried out far-UV CD spectroscopy of melittin in membranes of varying degrees of unsaturation. It is well established that monomeric melittin in aqueous solution shows essentially random coil conformation as reported earlier [6]. On the other hand, membrane-bound melittin shows a CD spectrum which is characteristic of an α-helical conformation [6,12,37]. The CD spectra of melittin bound to membranes composed of varying degrees of acyl chain unsaturation are shown in Fig. 7. Our result shows that melittin adopts α-helical conformation in mono- (POPC) and diunsaturated (PLPC) membranes and there is no significant difference in the α-helical content of melittin in these membranes. A slight shift is observed in the α-helical CD signature of melittin bound to PAPC membranes (Fig. 7). Importantly, a significant change (shift) in the CD spectrum of melittin is observed in case of melittin bound to PDPC membranes. The negative peak

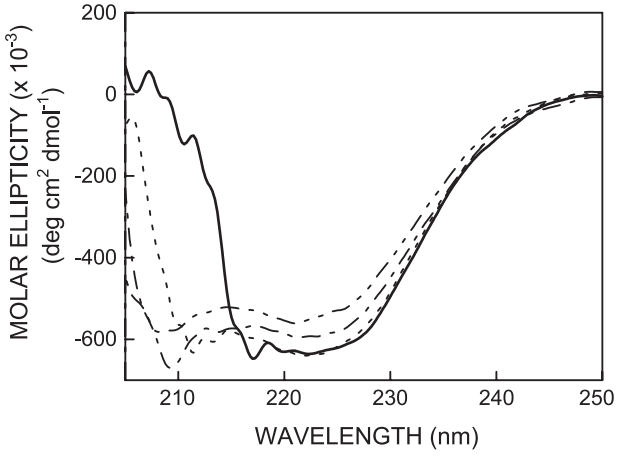

Fig. 7. Effect of increasing number of double bonds at the *sn*-2 fatty acyl chain on the far-UV CD spectra of melittin bound to membranes composed of varying degrees of unsaturation corresponding to POPC (— - -), PLPC (— - —), PAPC (– – –), and PDPC (—). The ratio of melittin to lipid was 1:50 (mol/mol) and the concentration of melittin was 17.0 μM in all cases. See Materials and methods for other details.

at 208 nm, characteristic of α-helical conformation, is lost and the resolution of the two negative peaks becomes less clear. Although the α-helix is considered to be the predominant secondary structural motif of membrane-bound melittin [6,12,37], the presence of a β-antiparallel pleated sheet has earlier been shown to exist for membrane-bound melittin [38]. Our results suggest that melittin, bound to highly unsaturated membranes such as PDPC membranes, could exhibit significantly different secondary structure. To the best of our knowledge, this is the first report showing such a change in the secondary structure of melittin in membranes of polyunsaturated phospholipids. Interestingly, it has been reported earlier that the last few residues at the carboxy terminal region (residues 23–26) of membrane-bound melittin are not part of the helix and are unfolded [39–41]. It is possible that in highly unsaturated membranes, there could be further unwinding of the helix resulting perhaps in an extended β-form. It should be noted here that although CD measurements are sensitive to sample scattering, these results are not influenced by scattering since the essential features of the CD spectra (such as relative peak positions) were found to be unaltered when lipid concentration was varied over a range (0.43–0.85 mM) keeping the peptide/lipid ratio constant at 1:50 (mol/mol).

4. Discussion

Membrane lipids play an important role in organizing biological membranes, mediating the formation of functional membrane domains, and modulating the structure and function of membrane proteins [42]. In particular, polyunsaturated lipids present in many biological membranes are of significant functional importance. Phospholipids with polyunsaturated acyl chains are known to influence membrane dynamics [30,36,43,44], and play an important role in regulating the structure and function of membrane peptides and proteins such as rhodopsin [45], and mechano-gated K^+ channels [46]. These studies point out the importance of lipid–protein interactions in modulating the function of membrane proteins, and demonstrate that lipid acyl chain unsaturation is an important factor in facilitating the structural organization and function of biological membranes. More importantly, polyunsaturated lipids have been reported to be crucial in health and disease [47].

In this paper, we have used the hemolytic peptide melittin to address the influence of unsaturated lipids in modulating lipid–protein interactions. In particular, we monitored the effect of increasing acyl chain unsaturation on membrane-bound melittin utilizing sensitive fluorescence-based approaches and CD spectroscopy. An interesting issue is the conformation of membrane-bound melittin in the experimental conditions used by us. As stated earlier, the orientation of membrane-bound melittin is dependent on a number of factors which include the physical condition and the composition of the membrane, and the concentration of the peptide [12,41]. Results from oriented CD spectroscopy measurements using melittin in fluid POPC bilayers show that the orientation of membrane-bound melittin is parallel to the membrane surface at melittin concentrations of 2.5 mol% (i.e. peptide/lipid ratios <1:40) or lower [12]. For example, at a peptide/lipid ratio of 1:40, melittin was found to be 85% parallel to the bilayer while this component is decreased to 68% at a peptide/lipid ratio of 1:15. In addition, the orientation of 1 mol% melittin in similar membranes have earlier been reported to be parallel to the membrane surface using a novel X-ray absolute scale refinement method [41]. These authors also reported, using oriented CD spectroscopy, that melittin starts reorienting perhaps to transmembrane orientation only at concentrations of ~4 mol%. Based on these results, it is reasonable to assume that melittin adopts an orientation parallel to the membrane surface under conditions reported in this paper.

Since phospholipids of most biological membranes are predominantly *sn*-1 saturated, *sn*-2 unsaturated acyl chains, we chose phospholipids with this general feature for this work. Our study assumes relevance due to the functional consequence (such as modulation of lytic ability and bilayer micellization) of the interaction of melittin with unsaturated membranes. Our results show that fluorescence parameters such as intensity, emission maximum, polarization, lifetime and acrylamide quenching of melittin incorporated in membranes are dependent on the degree of unsaturation of lipids in membranes. Importantly, melittin in membranes composed of various unsaturated lipids show REES implying that melittin is localized in a motionally restricted region in membranes. Interestingly, the extent of REES was found to increase drastically in membranes with increasing unsaturation, especially when the lipids contained more than two double bonds. The rotational mobility of melittin is considerably increased upon increasing the acyl chain unsaturation due to the loosening of inter-phospholipid packing near the lipid–water interface. In addition, time-resolved fluorescence and acrylamide quenching measurements reinforce the observation that the presence of unsaturation increases water penetration in the interfacial region of membranes composed of varying degrees of unsaturation. An interesting observation is that increasing unsaturation in membranes causes a considerable change in the secondary structure of membrane-bound melittin. In summary, our results assume significance in the overall context of the role of unsaturated lipids in membranes in the organization and function of membrane proteins and membrane-active peptides.

Acknowledgements

This work was supported by the Council of Scientific and Industrial Research, Government of India. We thank

Y.S.S.V. Prasad and G.G. Kingi for technical help, and members of our laboratory for critically reading the manuscript. H.R. thanks the Council of Scientific and Industrial Research for the award of a Senior Research Fellowship.

References

[1] C.E. Dempsey, The actions of melittin on membranes, Biochim. Biophys. Acta 1031 (1990) 143–161.
[2] T.C. Terwilliger, D. Eisenberg, The structure of melittin, J. Biol. Chem. 237 (1982) 6016–6022.
[3] C. Golding, P.O.' Shea, The interactions of signal sequences with membranes, Biochem. Soc. Trans. 23 (1995) 971–976.
[4] M. Rabenstein, Y.K. Shin, A peptide from the heptad repeat of human immunodeficiency virus gp41 shows both membrane binding and coiled-coil formation, Biochemistry 34 (1995) 13390–13397.
[5] K.J. Barnham, S.A. Monks, M.G. Hinds, A.A. Azad, R.S. Norton, Solution structure of polypeptide from the N terminus of the HIV protein Nef, Biochemistry 36 (1997) 5970–5980.
[6] A.K. Ghosh, R. Rukmini, A. Chattopadhyay, Modulation of tryptophan environment in membrane-bound melittin by negatively charged phospholipids: implications in membrane organization and function, Biochemistry 36 (1997) 14291–14305.
[7] T.D. Bradrick, A. Philippetis, S. Georghiou, Stopped-flow fluorometric study of the interaction of melittin with phospholipid bilayers: importance of the physical state of the bilayer and the acyl chain length, Biophys. J. 69 (1995) 1999–2010.
[8] H. Raghuraman, A. Chattopadhyay, Organization and dynamics of melittin in environments of graded hydration: a fluorescence approach, Langmuir 19 (2003) 10332–10341.
[9] H. Raghuraman, A. Chattopadhyay, Effect of micellar charge on the conformation and dynamics of melittin, Eur. Biophys. J. (2004) (in press).
[10] S.E. Blondelle, R.A. Houghten, Hemolytic and antimicrobial activities of twenty-four individual omission analogues of melittin, Biochemistry 30 (1991) 4671–4678.
[11] A. Chattopadhyay, R. Rukmini, Restricted mobility of the sole tryptophan in membrane-bound melittin, FEBS Lett. 335 (1993) 341–344.
[12] L. Yang, T.A. Harroun, T.M. Weiss, L. Ding, H.W. Huang, Barrel-stave model or toroidal model? A case study on melittin pores, Biophys. J. 81 (2001) 1475–1485.
[13] M. Monette, M. Lafleur, Modulation of melittin-induced lysis by surface charge density of membranes, Biophys. J. 68 (1995) 187–195.
[14] T. Benachir, M. Monette, J. Grenier, M. Lafleur, Melittin-induced leakage from phosphatidylcholine vesicles is modulated by cholesterol: a property used for membrane targeting, Eur. Biophys. J. 25 (1997) 201–210.
[15] N.K. Subbarao, R.C. MacDonald, Lipid unsaturation influences melittin-induced leakage of vesicles, Biochim. Biophys. Acta 1189 (1994) 101–107.
[16] M. Monette, M. Lafleur, Influence of lipid chain unsaturation on melittin-induced micellization, Biophys. J. 70 (1996) 2195–2202.
[17] A. Chattopadhyay, Exploring membrane organization and dynamics by the wavelength-selective fluorescence approach, Chem. Phys. Lipids 122 (2003) 3–17.
[18] J.C. Dittmer, R.L. Lester, Simple, specific spray for the detection of phospholipids on the thin-layer chromatograms, J. Lipid Res. 5 (1964) 126–127.
[19] C.W.F. McClare, An accurate and convenient organic phosphorus assay, Anal. Biochem. 39 (1971) 527–530.
[20] R.A. Klein, The detection of oxidation in liposome preparations, Biochim. Biophys. Acta 210 (1970) 486–489.
[21] M.R. Eftink, Fluorescence quenching reactions: probing biological macromolecular structure, in: T.G. Dewey (Ed.), Biophysical and Biochemical Aspects of Fluorescence Spectroscopy, Plenum, New York, 1991, pp. 1–41.
[22] R.C. MacDonald, R.I. MacDonald, B.P. Menco, K. Takeshita, N.K. Subbarao, L.R. Hu, Small-volume extrusion apparatus for preparation of large, unilamellar vesicles, Biochim. Biophys. Acta 1061 (1991) 297–303.
[23] J.R. Lakowicz, Principles of Fluorescence Spectroscopy, Plenum, New York, 1999.
[24] R.B. Gennis, Biomembranes: Molecular Structure and Function, Springer-Verlag, New York, 1989, p. 26.
[25] K. Olbrich, W. Rawicz, D. Needham, E. Evans, Water permeability and mechanical strength of polyunsaturated lipid bilayers, Biophys. J. 79 (2000) 321–327.
[26] D. Huster, A.J. Jin, K. Arnold, K. Gawrisch, Water permeability of polyunsaturated lipid membranes measured by ^{17}O NMR, Biophys. J. 73 (1997) 855–864.
[27] A.P. Demchenko, The red-edge effects: 30 years of exploration, Luminescence 17 (2002) 19–42.
[28] P. Mentré (Ed.), Water in the Cell, Cell. Mol. Biol. 47 (2001) 709–970.
[29] S.H. White, W.C. Wimley, Peptides in lipid bilayers: structural and thermodynamic basis for partitioning and folding, Curr. Opin. Struct. Biol. 4 (1994) 79–86.
[30] L. Saiz, M.L. Klein, Influence of highly polyunsaturated lipid acyl chains of biomembranes on the NMR order parameters, J. Am. Chem. Soc. 123 (2001) 7381–7387.
[31] M.C. Tory, A.R. Merrill, Determination of membrane protein topology by red-edge excitation shift analysis: application to the membrane-bound colicin E1 channel peptide, Biochim. Biophys. Acta 1564 (2002) 435–448.
[32] N.C. Santos, M. Prieto, M.A. Castanho, Interaction of the major epitope region of HIV protein gp41 with membrane model systems. A fluorescence spectroscopy study, Biochemistry 37 (1998) 8674–8682.
[33] L.A. Falls, B.C. Furie, M. Jacobs, B. Furie, A.C. Rigby, The omega-loop region of the human prothrombin gamma-carboxyglutamic acid domain penetrates anionic phospholipid membranes, J. Biol. Chem. 276 (2001) 23895–23905.
[34] E.P. Kirby, R.F. Steiner, The influence of solvent and temperature upon the fluorescence of indole derivatives, J. Phys. Chem. 74 (1970) 4480–4490.
[35] W. Rawicz, K.C. Olbrich, T. McIntosh, D. Needham, E. Evans, Effects of chain length and unsaturation on elasticity of lipid bilayers, Biophys. J. 79 (2000) 328–339.
[36] L.L. Holte, S.A. Peter, T.M. Sinnwell, K. Gawrisch, ^{2}H nuclear magnetic resonance order parameter profiles suggest a change of molecular shape for phosphatidylcholines containing a polyunsaturated acyl chain, Biophys. J. 68 (1995) 2396–2403.
[37] A.S. Ladokhin, S.H. White, Folding of amphipathic α-helices on membranes: energetics of helix formation by melittin, J. Mol. Biol. 285 (1999) 1363–1369.
[38] J.W. Brauner, R. Mendelsohn, F.G. Prendergast, Attenuted total reflectance Fourier transform infrared studies of the interaction of melittin, two fragments of melittin, and delta-hemolysin with phosphatidylcholines, Biochemistry 26 (1987) 8151–8158.
[39] C.E. Dempsey, G.S. Butler, Helical structure and orientation of melittin in dispersed phospholipid membranes from amide exchange analysis in situ, Biochemistry 31 (1992) 11973–11977.
[40] A. Okada, K. Wakamatsu, T. Miyazawa, T. Higashijima, Vesicle-bound conformation of melittin: transferred nuclear Overhauser enhancement analysis in the presence of perdeuterated phosphatidylcholine vesicles, Biochemistry 33 (1994) 9438–9446.
[41] K. Hristova, C.E. Dempsey, S.H. White, Structure, location and lipid perturbations of melittin at the membrane interface, Biophys. J. 80 (2001) 801–811.
[42] A.G. Lee, Lipid–protein interactions in biological membranes: a structural perspective, Biochim. Biophys. Acta 1612 (2003) 1–40.

[43] A. Salmon, S.W. Dodd, G.D. Williams, J.M. Beach, M.F. Brown, Configurational statistics of acyl chains in polyunsaturated lipid bilayers from ^{2}H NMR, J. Am. Chem. Soc. 109 (1987) 2600–2609.
[44] D.C. Mitchell, B.J. Litman, Molecular order and dynamics in bilayers consisting of highly polyunsaturated phospholipids, Biophys. J. 74 (1998) 879–891.
[45] B.J. Litman, D.C. Mitchell, A role of phospholipid polyunsaturation in modulating membrane protein function, Lipids 31 (1996) S193–S197.
[46] A.J. Patel, M. Lazdunski, E. Honoré, Lipid and mechano-gated 2P domain K^{+} channels, Curr. Opin. Cell Biol. 13 (2001) 422–427.
[47] S.D. Freedman, M.H. Katz, E.M. Parker, M. Laposata, M.Y. Urman, J.G. Alvarez, A membrane lipid imbalance plays a role in the phenotypic expression of cystic fibrosis in *cftr*$^{-/-}$ mice, Proc. Natl. Acad. Sci. U. S. A. 96 (1999) 13995–14000.